MOLECULAR PHYSICS REPORTS **38** (2003) 118-123

XPS STUDIES OF NANOCRYSTALLINE AND POLYCRYSTALLINE $LaNi_5$ THIN FILMS

L. SMARDZ[1], K. SMARDZ[2], M. NOWAK[2], M. JURCZYK[2]

[1] *Institute of Molecular Physics, Polish Academy of Sciences, Smoluchowskiego 17, 60-179 Poznań, Poland*

[2] *Institute of Materials Sciences and Engineering, Poznań University of Technology, M. Curie 5 Sq., Poznań, Poland*

Abstract: $LaNi_5$ alloy thin films were prepared onto glass substrates in the temperature range 285-700 K using computer-controlled ultra high vacuum (UHV) magnetron co-sputtering. Ni and La targets were sputtered using DC and RF modes, respectively. The chemical composition and the cleanness of all layers was checked *in-situ*, immediately after deposition, transferring the samples to an UHV (4×10^{-11} mbar) analysis chamber equipped with XPS. The bulk nanocrystalline and polycrystalline $La(Ni, Al)_5$ alloys were prepared using mechanical alloying followed by annealing and arc melting method, respectively. Structural studies showed that the $LaNi_5$ thin films deposited at 295 K are nanocrystalline with average grain size $D \sim 15$ nm. Thin films deposited at about 700 K are polycrystalline with $D \sim 200$ nm. The different microstructure observed in polycrystalline and nanocrystalline $LaNi_5$-type alloys prepared as a bulk material or thin film leads to significant modifications of the electronic structure of the intermetallic.

1. INTRODUCTION

A large number of experimental investigation on $LaNi_5$ and related compounds have been performed up to now in relation to their exceptional hydrogenation properties [1]. In order to optimise the choice of the intermetallic compounds for a selected application, a better understanding of the role of each alloy constituent on the electronic properties of the material is crucial. Several semi-empirical models [2, 3] have been proposed for the heat of formation and heat of solution of metal hydrides and attempts have been made for justifying the maximum hydrogen absorption capacity of the metallic matrices. These models showed that the energy of the metal-hydrogen interaction depend both on geometric and electronic factors. In this contribution, we study experimentally the electronic properties of polycrystalline and nanocrystalline $LaNi_5$ thin films using X-ray photoelectron spectroscopy (XPS). For a comparison we will also show XPS results for bulk nanocrystalline and polycrystalline $LaNi_5$-type alloys. The structure of the samples has been studied by X-ray diffraction (XRD). Their bulk chemical compositions were measured using X-ray fluorescence (XRF) method. The scanning electron microscopy (SEM) technique was used to follow the changes in size and shape of the grains. These measurements may supply useful indirect information about the influence of the electronic structure of polycrystalline and nanocrystalline $LaNi_5$-type alloys on their hydrogenation properties.

2. EXPERIMENTAL PROCEDURE

$LaNi_5$ alloy thin films were prepared onto glass substrates in the temperature range 285-700 K using computer-controlled ultra high vacuum (UHV) magnetron co-sputtering. Ni and La targets

were sputtered using DC and RF modes, respectively. The base pressure before the deposition process was lower than 5×10^{-10} mbar. The chemical composition and the cleanness of all layers was checked *in-situ*, immediately after deposition, transferring the samples to an UHV (4×10^{-11} mbar) analysis chamber equipped with XPS [4]. The XPS spectra were measured with Al-K_α radiation at 1486.6 eV at room temperature using a SPECS EA 10 PLUS energy spectrometer. All emission spectra were measured immediately after *in-situ* sample transfer in a vacuum of 8×10^{-11} mbar. The deposition rates of La and Ni and $LaNi_5$ thin films are individually checked by a quartz thickness monitors. The total thickness of the samples was about 1000 nm. The assumed thickness and composition of the deposited films were also revealed by X-ray fluorescence analysis (XRF). Typical sputtering conditions used during the deposition of $LaNi_5$ alloy thin films were collected in Table I.

Table I. Typical sputtering conditions used for deposition of $LaNi_5$ thin films

Parameter	Unit	La	
Rest gas pressure	mbar	5×10^{-10}	
Argon partial pressure	mbar	5×10^{-4}	
Argon purity	%	99.9998	
Target diameter	mm	51.5	
Target purity	%	99.99	99.999
Distance between substrate and target	mm	220	
Sputtering method		Magnetron RF	Magnetron DC
Sputtering power	W	75	60
Deposition rate	Nm/s	0.04	0.1
Substrate temperature during deposition	K	295 (nanocrystalline) 700 (polycystalline)	

The polycrystalline $La(Ni, Al)_5$ alloys were prepared by arc melting stoichiometric amounts of the constituent elements (purity 99.9% or better) in a high purity argon atmosphere. The as cast ingot was homogenised at 1170 K for 3 days and then rapidly cooled to room temperature in water. The nanocrystalline $La(Ni, Al)_5$ alloys were prepared using mechanical alloying (MA) followed by annealing. MA was performed under argon atmosphere using a SPEX 8000 Mixer Mill.

3. RESULTS AND DISCUSSION

Structural studies showed that the $LaNi_5$ thin films deposited at 295 K are nanocrystalline with average grain size $D \sim 15$ nm. Thin films deposited at about 700 K are polycrystalline with $D \sim 200$ nm.

The MA process has been studied by X-ray diffraction and microstructural investigations, using $LaNi_{4.2}Al_{0.8}$ as representative alloy example. Figure 1 shows a series of XRD spectra of mechanically alloyed La-Ni-Al mixture (34.13 wt% of La, 60.57 wt% of Ni and 5.30 wt% of Al) subjected to milling in increasing time, respectively. The originally sharp diffraction lines of La, Ni and Al (Fig. 1a) gradually become broader and their intensity decreases with milling time. The powder mixture milled for more than 40 h has transformed completely to the amorphous

phase (see Fig. 1b). It is worth noting that before amorphisation no shift of the La, Ni and Al diffraction lines was observed. This result means that the amorphous phase forms directly from the starting mixture of the elements (La, Ni and Al), without formation of an other phase. Using the La-Ni-Al mixture composition, as the representative material example, the behaviour of the grain size of the crystallites has been studied during the mechanical alloying process. The Ni (111) diffraction line remains visible up to 15 h of milling. This allows an estimation of the change in the crystallite size of Ni with increasing of the milling time. The crystallite size decreases strongly from 50 nm at the beginning of the mechanical alloying process. The final size of crystallites, about 33 nm, seems to be favourable to the formation of an amorphous phase, which develops at the La-Ni-Al interfaces. Further milling significantly weakens the diffraction peak intensity so that it is impossible to estimate the crystallite size. Formation of nanocrystalline $LaNi_{4.2}Al_{0.8}$ alloy was achieved by annealing the amorphous materials in high purity argon atmosphere at 1070 K for 1 h (Fig. 1c). All diffraction peaks were assigned to those of the hexagonal crystal structure of $CaCu_5$-type with cell parameters $a = 5.056$ Å and $c = 4.007$ Å. After hydrogenation at room temperature, each peak was shifted, indicating that the lattices undergoes a volume expansion of 19% (Fig. 1d). Results show that the amorphous phase of MA samples forms directly from the starting mixture of the elements, without other phase formation. Heating the MA powders at 1070 K for 1 h resulted in the creation of hexagonal $CaCu_5$-type nanocrystalline compound with mean crystallite size less than 30 nm. The average grain size of the polycrystalline sample was about 250 nm.

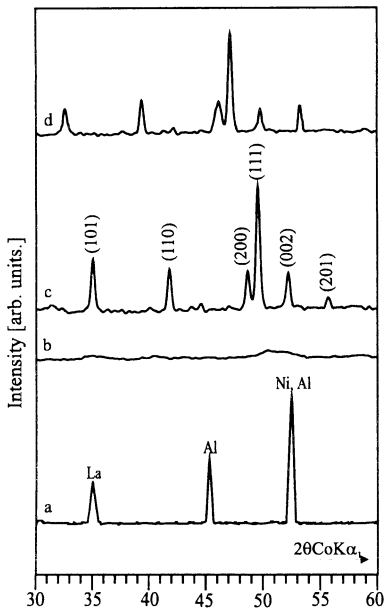

Fig. 1. XRD spectra of a mixture of La, Ni and Al powders mechanically alloyed for different times in an argon atmosphere: (a) initial state (elemental powder mixture), (b) after MA for 40 h, (c) heat treated at 1070 K for 1 h and (d) hydrogenated

Figure 2 shows XPS spectrum of the freshly prepared nanocrystalline 1000 nm – $LaNi_5$ thin film. The sample was deposited after the outgasing procedure of the glass substrate with holder at 700 K for 3 h. For a comparison we show results for the nanocrystalline $LaNi_5$ bulk alloy.

The spectrum of the thin film was measured *in-situ*, immediately after deposition. The bulk sample was prepared *ex-situ* by MA followed by annealing in a high-purity argon atmosphere. The bulk nanocrystalline $LaNi_5$ was measured immediately after heating in UHV conditions followed by removing of a native oxide and possible impurities layer using ion gun etching system. The XPS intensity of the MA nanocrystalline alloy is considerably reduced compared to that measured for thin film. This is due to not perfectly clean surface and significantly greater roughness parameter of the bulk alloy. The oxygen concentration on the surface is about 0.1 and 2 at.% for nanocrystalline $LaNi_5$ thin film and MA bulk alloy, respectively. The XPS measurements after removing of the 50 nm top $LaNi_5$ layer revealed the same oxygen concentration in the MA sample while practically no trace of oxygen atoms in the thin film volume. Average roughness parameter determined by scanning tunnelling microscopy was about 1 and 100 nm for nanocrystalline $LaNi_5$ thin film and MA bulk alloy, respectively.

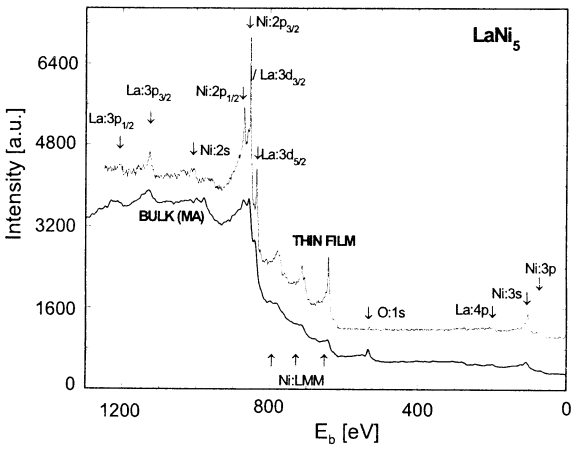

Fig. 2. XPS spectrum of the freshly prepared nano-crystalline 1000 nm – $LaNi_5$ thin film. For a comparison we show results for the nanocrystalline $LaNi_5$ bulk alloy

In Figure 3 we show the XPS valence bands for nanocrystalline (bold solid line) and polycrystalline (thin solid line) $LaNi_5$ films. For a comparison we show in Fig. 3 also results for the nanocrystalline and polycrystalline $LaNi_{4.2}Al_{0.8}$ bulk alloys represented by bold and thin broken lines, respectively. The spectra of the thin films were measured in-situ, immediately after deposition. The bulk samples were measured immediately after heating in UHV conditions followed by removing of a native oxide and possible impurities layer using ion gun etching system.

We have found very good agreement between experimental results for polycrystalline $LaNi_5$ thin film (thin solid line in Fig. 3) and *ab-initio* LMTO calculations of the total density of states (DOS) [5]. The occupied part of the conduction band is dominated by the Ni 3*d* states with a non-negligible bonding contribution of the La-5*d* states. The main part of the La-5*d* states is located above the Fermi energy [5]. The XPS signal at E_F is high and mostly composed of Ni-*d* states since the La-5*d* contribution is practically negligible [5]. In spite of the large value of the DOS at E_F $LaNi_5$ is a Pauli paramagnet. The shape of the valence band measured for the polycrystalline $LaNi_5$ thin film is practically the same compared to that reported earlier for the single crystalline sample [1]. On the other hand, the XPS valence band of the nanocrystalline $LaNi_5$ thin film (bold

solid line) is considerably broader compared to that measured for the polycrystalline sample. This is probably due to a strong deformation of the nanocrystals. Normally the interior of the nanocrystal is constrained and the distances between atoms located at the grain boundaries expanded [6-8]. Similar broadening of the valence band can be also observed for the MA nanocrystalline $LaNi_{4.2}Al_{0.8}$ bulk alloy (bold broken line) compared to that measured for the polycrystalline bulk sample (thin broken line).

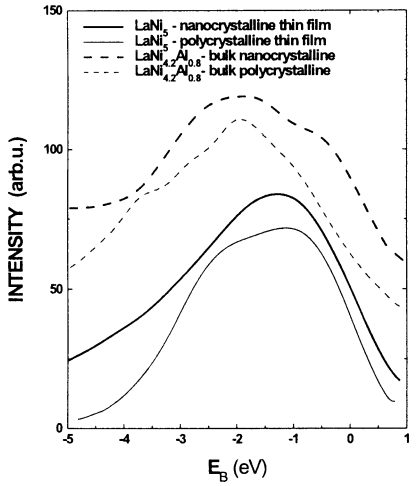

Fig. 3. XPS valence band spectra for nanocrystalline (bold solid line) and polycrystalline (thin solid line) $LaNi_5$ thin films using Al-K_α radiation. Results for the nanocrystalline and polycrystalline $LaNi_{4.2}Al_{0.8}$ bulk alloys are represented by bold and thin broken lines, respectively

$LaNi_5$-based materials combine a high reversible energy storage capacity with fast electrochemical activation, excellent long term cycling stability and good charge/discharge kinetics, making Ni-MH_x batteries nowadays a serious alternative for Ni-Cd batteries. The properties of hydrogen host materials can be modified substantially by alloying, to obtain the desired storage characteristics e.g. proper capacity at a favourable hydrogen pressure. As discovered earlier, the alloy element such as Al substituted for Ni in nanocrystalline $MmNi_5$ (Mm – mischmetal) type alloys greatly improved the activation behaviour of nanocrystalline electrode [9]. The use of mischmetal instead lanthanum was performed mainly from economical point of view. The discharge capacity of $MmNi_5$ was only 37 mAh g^{-1}. For nanocrystalline $MmNi_{4.2}Al_{0.8}$ material we have found that the discharge capacity as large as 207 mAh g^{-1} at current density of charging and discharging of 40 mA g^{-1} (note, that the lanthanum content in mischmetal was only 25 wt.%) [9]. Recently, we have also reported the pressure-composition isotherms for desorption of hydrogen from gas phase, at room temperature, on nanocrystalline as well as polycrystalline $LaNi_{4.2}Al_{0.8}$ materials [10]. Results showed that the isotherms of nanocrystalline material differ significantly from the polycrystalline material, for which enhancement of solid state solubility is observed. It was also observed that the amount of absorbed hydrogen at a pressure of 1.1 MPa decreases for nanocrystalline material. The significant modification of the electronic structure of the nanocrystalline material (see Fig. 3) could be responsible for the observed hydrogenation properties. On the other hand, it is not excluded that another factor such as Fe surface impurities of MA samples due to degradation of milling media [11], could also influence on the hydrogenation process of nanocrystalline $LaNi_{4.2}Al_{0.8}$.

4. CONCLUSION

The different microstructure observed in polycrystalline and nanocrystalline $LaNi_5$-type alloys prepared as a bulk material or thin film leads to significant modifications of the electronic structure of the intermetallic. Such a modification of the electronic structure of the nanocrystalline $LaNi_5$-type alloy compared to that of polycrystalline sample could significantly influence on its hydrogenation properties.

Acknowledgements

The financial support from the Polish National Committee for Scientific Research (KBN) under the contract No PBZ-KBN-013/T08/02 is gratefully acknowledged. The UHV equipment for surface analyses used for the XPS and AES measurements and glove box Labmaster 130 (M. Braun) were purchased by the Foundation for Polish Science under the program SEZAM-94 and TECHNO-2000, respectively.

References

[1] L. Schlapbach, *Hydrogen in Intermetallic Compounds*, II, Springer, Berlin, 1992, p. 165.
[2] P. C. Bouten, A. R. Miedema, J. Less Common Metals **71**, 147 (1980).
[3] R Griessen, Phys. Rev. **B38,** 3690 (1988).
[4] L. Smardz, K. Smardz, M. Jurczyk, J. Jakubowicz, J. Alloy Comp. **313**, 192 (2000).
[5] A. Szajek, L. Smardz, M. Jurczyk, K. Smardz, M. Nowak, Czech. J. Phys. **52**, suppl. A209 (2002).
[6] L. Smardz, K. Le Dang, H. Niedoba, K. Chrzumnicka, J. Magn. Magn. Mater. **140-144**, 569 (1995).
[7] L. Smardz, K. Smardz, R. Czajka, Cryst. Res. Technol **36**, 1019 (2001).
[8] L. Smardz, K. Smardz, R. Czajka, phys. stat. sol. **a 196**, 173 (2003).
[9] M. Jurczyk, W. Rajewski, W. Majchrzycki, G. Wojcik, J. Alloys Comp. **290**, 264 (1999).
[10] M. Jurczyk, K. Smardz, W. Rajewski, L. Smardz, Mater. Sci. & Engin. **A303**, 70 (2001).
[11] L. Smardz, M. Jurczyk, K. Smardz, M. Nowak, Czech. J. Phys. **52**, suppl. **A177**, (2002).